# Wavelet Galerkin Methods for Elastic Multibody Systems

Diaz, José; Führer, Claus

*Published in:*
European Congress on Computational Methods in Applied Sciences and Engineering ECCOMAS

2004

European Congress on Computational Methods in Applied Sciences and Engineering
ECCOMAS 2004
P. Neittaanmäki, T. Rossi, S. Korotov, E. Oñate, J. Périaux, and D. Knörzer (eds.)
Jyväskylä, 24–28 July 2004

# WAVELET GALERKIN METHODS FOR ELASTIC MULTIBODY SYSTEMS - A CASE STUDY: ROLLER BEARINGS.

**José Díaz López, Claus Führer**

Numerical Analysis
Lund University
Box 118, SE-211 00 Lund, Sweden
e-mail: {jose,claus}@maths.lth.se, web page: http://www.maths.lth.se/na

**Key words:** Galerkin, Wavelet, Elasticity, Roller Bearings

**Abstract.** *In the present paper we discuss simulation with a wavelet element method. The model problem is a simplified 2D-roller bearing model consisting of an elastic outer and inner ring and a roller. This model reflects typical properties of elastic multibody systems, eg. combination of gross motion with elastic deformation and contact problems. The wavelet element method is implemented in a similar way as the widely used finite element method. Its inherent advantages concerning model reduction will be demonstrated as well as the influence of model reduction on simulation time.*

## 1 Elastic Roller Bearing Model Problem

In order to demonstrate the power of a wavelet element method we consider an elastic extension of a simplified 2D-roller bearing model presented in [11]. The model consists of two elastic rings and an elastic roller see Fig. 1. The outer ring is assumed to rotate

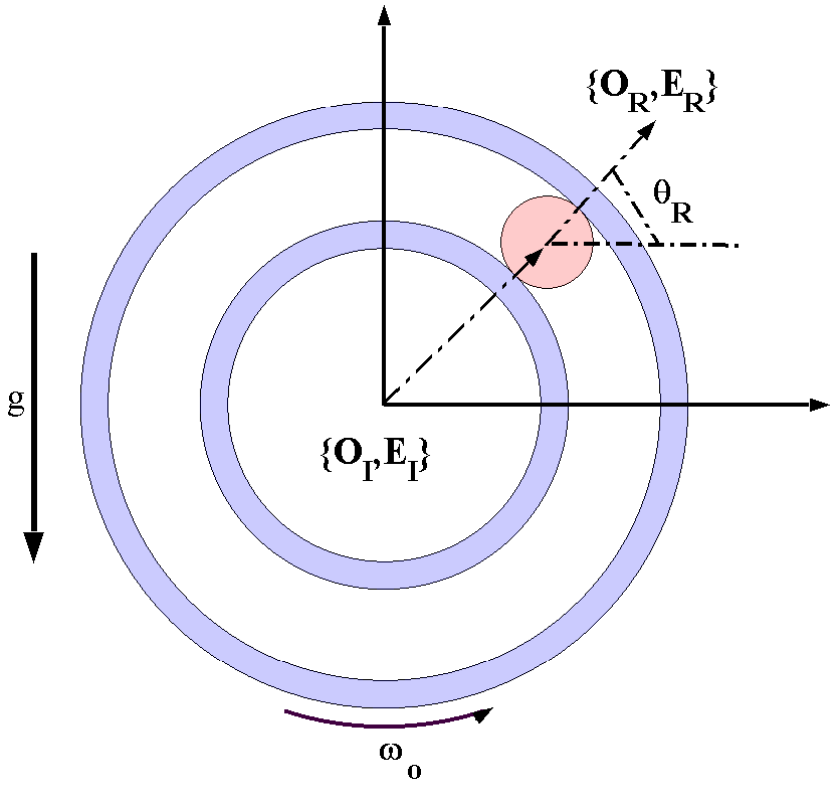


Figure 1: 2D roller bearing model and rigid body states

with constant speed $\omega_o$, while the inner ring is fixed. The rollers may be in contact with one of the rings depending on their state. The inertial system is placed into the center of the inner ring and the outer ring is described by means of Cartesian coordinates with respect to that system by the six rigid state variables $(y_{\text{out}}, \theta_{\text{out}}, \dot{y}_{\text{out}}, \theta_{\text{out}})$, where $y \in \mathbb{R}^2$ expresses the coordinates of the center of the outer ring and $\theta$ its orientation. The motion of the roller is given accordingly by the rigid states $(y_{\text{R}}, \theta_{\text{R}}, \dot{y}_{\text{R}}, \theta_{\text{R}})$.

The elastic deformation is taken into account by additional elastic state variables, $q_{\text{R}}, \dot{q}_{\text{R}} \in \mathbb{R}^{N_{\text{R}}}$ for the roller and $q_{\text{out}}, \dot{q}_{\text{out}} \in \mathbb{R}^{N_{\text{out}}}$, $q_{\text{in}}, \dot{q}_{\text{in}} \in \mathbb{R}^{N_{\text{in}}}$ for the rings, resulting from a wavelet semidiscretization of the rollers and the rings.

The total number of elastic degrees of freedom depends on the discretization and is normally substantially larger than the number of rigid degrees of freedom.

The number of elastic degrees of freedom is classically reduced when using a finite element discretization by modal reduction techniques. Using modal reduction techniques to reduce the number of elastic degrees of freedom may yield a poor description of the relevant quantities for multibody simulation, e.g. direction and magnitude of the contact forces.

In contrast, semidiscretization by wavelets offers direct reduction possibilities while preserving the description of the deformation field near the contact point which yields better results and speeds up the simulation time.

The disposition of the paper is the following: In Section 2 we present the equations of motion of a single elastic body. In Sec. 3 a brief introduction to wavelets and the wavelet element method (WEM) adapted to our model problem is presented. In Sec. 4 the contact interaction is discussed and included in the model. Numerical simulations are presented in Sec. 6.

## 2 ELASTIC BODY MOTION

The coupled elastic/rigid motion is described here for the outer ring. The description of the inner ring and the roller follows in a similar way. All three elastic bodies are then coupled together by contact constraints.

The body has the reference configuration $\bar{\Omega}$, which is the closure of an open convex set $\Omega \in \mathbb{R}^2$ with the boundary $\Gamma$. We assume that this boundary is divided into two disjoint sections $\Gamma_0$ and $\Gamma_1$ and will impose Dirichlet (natural) boundary conditions at $\Gamma_0$ and Neumann (essential) boundary conditions at $\Gamma_1$.

The body's deformation is described in material coordinates, i.e. with respect to the reference configuration of the undeformed body with the displacement field $u(x,t), \quad x \in \Omega$, see Fig. 2.

For a fixed time $t$ the displacement field $u$ is a function in the Hilbert space

$$\mathcal{V} = \left\{ \mathbf{v} : v_i \in H^1(\Omega), i = 1,2,3 \right\}$$

with the inner product

$$\langle v, w \rangle_{\mathcal{V}} = \sum_{i=1}^{2} \langle v_i, w_i \rangle_{H^1} .$$

As we will state following the lines of the equations of motion in their weak or variational form, [10], we have to consider also the subspace of test functions

$$\mathcal{V}_0 = \{ \mathbf{v} \in \mathcal{V} : \mathbf{v}|_{\Gamma_0} = 0 \} .$$

With the body's mass $m$, moment of inertia $J(u) = \int_\Omega \rho(x+u)^T(x+u)\mathrm{d}x$, constant density $\rho$, inner volume forces $\beta(x,\theta)$ and surface forces $\tau(x,\theta)$ on $\Gamma_1$ the equations of

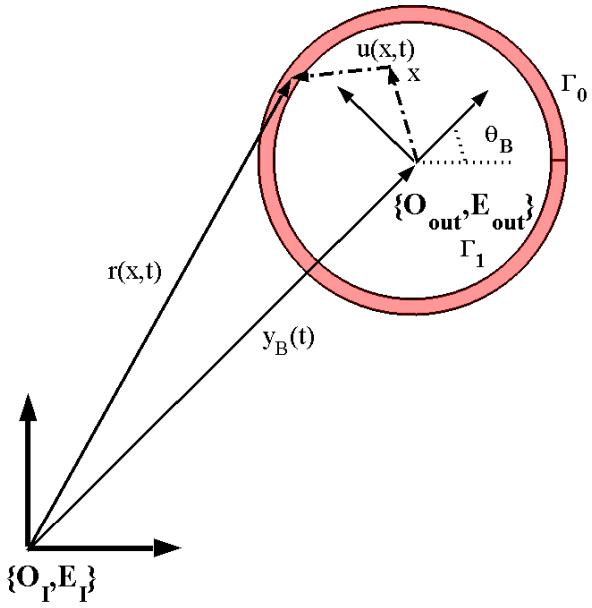


Figure 2: Reference systems in an elastic body

motion of the outer ring take the form:

$$m\ddot{y} + A'(\theta)s(u)\ddot{\theta} - A(\theta)s(u)\dot{\theta}^2 + 2A'(\theta)\dot{\theta}\int_\Omega \rho\dot{u}\mathrm{d}x = A\int_\Omega \beta(x,\theta)\mathrm{d}x + A(\theta)\int_{\Gamma_1}\tau(x,\theta)\mathrm{d}s \quad (1a)$$

$$s(u)^{\mathrm{T}}A'(\theta)^{\mathrm{T}}\ddot{y} + J\ddot{\theta} + \int_\Omega \rho(x+u)^{\mathrm{T}}\tilde{\mathrm{I}}\ddot{u}\mathrm{d}x + 2\dot{\theta}\int_\Omega \rho(x+u)^{\mathrm{T}}\dot{u}\mathrm{d}x = \int_\Omega (x+u)^{\mathrm{T}}\tilde{\mathrm{I}}\beta(x,\theta)\mathrm{d}x + \int_{\Gamma_1}(x+u)^{\mathrm{T}}\tilde{\mathrm{I}}\tau(x,\theta)\mathrm{d}s \quad (1b)$$

$$\left\langle \rho A(\theta)^{\mathrm{T}}\ddot{y}, v\right\rangle + \left\langle \rho(\ddot{\theta}\tilde{\mathrm{I}}^{\mathrm{T}} - \dot{\theta}\mathrm{I})(x+u), v\right\rangle + \left\langle \rho(2\tilde{\mathrm{I}}^{\mathrm{T}}\dot{u}\dot{\theta}), v\right\rangle + \langle \rho\ddot{u}, v\rangle + \mathrm{a}(u,v) = \langle l, v\rangle, \forall v \in \mathcal{V}_0, \quad (1c)$$

where $A(\theta)$ is the 2D rotation matrix, $s(u) = \int_\Omega \rho(x+u)\mathrm{d}x$, and $\tilde{\mathrm{I}} = \begin{pmatrix} 0 & -1 \\ 1 & 0 \end{pmatrix}$. $\mathrm{a}(u,v)$ is the bilinear form depending on the constitutive elasticity law and $\langle v, l\rangle$ a linear form arising form homogeneisation of boundary conditions at $\Gamma_o$.

For more details, see [10, 8].

### 2.0.1 Galerkin Semidiscretisation

Consider now a finite dimensional subspace $\mathcal{V}_0^h \subset \mathcal{V}_0$ with a basis $\{\zeta_j\}_{j=1}^{N_q}$. Galerkin semidiscretization seeks for an approximative solution $u^h \in \mathcal{V}_0^h$. A special case is the wavelet element method which takes a wavelet basis $\{\zeta_j\}_{j=1}^{N_q}$ for $\mathcal{V}_0^h$.

The usual separation ansatz leads to

$$u^h(x,t) = \sum_{j=1}^{N_q} q_j(t)\zeta_j(x)$$

with a set of time dependent coefficients $\{q_j(t)\}_j$, the elastic states of the system. To compactify the presentation we write

$$u^h(x,t) = N(x)q(t) = \big(\zeta_1(x)...\zeta_j(x)...\zeta_{N_q}(x)\big) \begin{pmatrix} q_1 \\ \vdots \\ q_j \\ \vdots \\ q_{N_q} \end{pmatrix}.$$

We obtain then $N+3$ differential equations to determine $y, \theta$ and $q$:

$$m\ddot{y} + A'\left(s_r + s_h q\right)\ddot{\theta} + AC_1^{\mathrm{T}}\ddot{q} = A\left(s_r + s_h q\right)\dot{\theta}^2 - 2A'C_1^{\mathrm{T}}\dot{q} + f_{\mathrm{T}}(\theta, q, t) \tag{2a}$$

$$\left(s_r + s_h q\right)A'^{\mathrm{T}}\ddot{y} + \left(J_r + J_h q\right)\ddot{\theta} + \left(C_2 + C_3 q\right)\ddot{q} = -2\left(C_4 + M_h q\right)\dot{\theta}\dot{q} + f_R(\theta, q, t) \tag{2b}$$

$$C_1 A^{\mathrm{T}}\ddot{y} + (C_2 + C_3(q))\ddot{\theta} + M_h\ddot{q} = (C_4 + M_h q)\dot{\theta}^2 - 2C_3\dot{\theta}\dot{q} - K_h q + l_h \tag{2c}$$

where we introduced the following abbreviations:

- **Discrete mass, stiffness matrix and forces**

$$\begin{aligned} M_h &= \int_\Omega \rho N^{\mathrm{T}} N \mathrm{d}x \\ (K_h)_{j_1,j_2} &= \mathrm{a}(\zeta_{j_1}, \zeta_{j_2}) \\ (l_h)_j &= \langle l, \zeta_j \rangle \end{aligned}$$

- **Coupling matrices**

$$\begin{aligned} C_1 &= \int_\Omega \rho N^{\mathrm{T}} \mathrm{d}x, & C_2 &= \int_\Omega \rho(x_1 N_2 - x_2 N_1)\mathrm{d}x \\ C_3 &= \int_\Omega \rho(N_2^{\mathrm{T}} N_1 - N_1^{\mathrm{T}} N_2)\mathrm{d}x, & C_4 &= \int_\Omega \rho(x_1 N_1 + x_2 N_2)\mathrm{d}x \end{aligned}$$

- **Variation terms**

$$s_h \;=\; \int_\Omega \rho N \mathrm{d}x, \qquad J_h \;=\; 2C_4 q + q^{\mathrm{T}} M_h q$$

- **Force terms**

$$\begin{aligned} f_T(\theta,t) &= A\int_\Omega \beta(x,\theta)\mathrm{d}x + A\int_{\Gamma_1}\tau(x,\theta)\mathrm{d}x \\ f_R(\theta,q,t) &= \int_\Omega (x+Nq)^{\mathrm{T}}\tilde{\mathrm{I}}\beta(x,\theta)\mathrm{d}x + \int_{\Gamma_1}(x+Nq)^{\mathrm{T}}\tilde{\mathrm{I}}\tau(x,\theta)\mathrm{d}x \end{aligned}$$

### 2.1 Semidiscretized Roller Bearing system

We collect the degrees of freedom in a state vector $w = \left(q_{\mathrm{in}},\ \ w_{\mathrm{R}},\ \ w_{\mathrm{out}}\right)^{\mathrm{T}}$ with the states for the roller and outer ring $w_{\mathrm{R/out}} = \left(y_{\mathrm{R/out}},\ \ \theta_{\mathrm{R/out}},\ \ q_{\mathrm{R/out}}\right)^{\mathrm{T}}$.

The motion of the uncoupled system is then described the by differential equations

$$\begin{pmatrix} M_{\mathrm{in}} & & \\ & M_{\mathrm{R}} & \\ & & M_{\mathrm{out}} \end{pmatrix} \ddot{w} = \begin{pmatrix} f_{\mathrm{in}}(t, w_{\mathrm{in}}, \dot{w}_{\mathrm{in}}) \\ f_{\mathrm{R}}(t, w_{\mathrm{R}}, \dot{w}_{\mathrm{R}}) \\ f_{\mathrm{out}}(t, w_{\mathrm{out}}, \dot{w}_{\mathrm{out}}) \end{pmatrix}$$

where the matrices for the roller and outer ring $i \in \{\mathrm{R}, \mathrm{out}\}$ are

$$M_i(w_i) = \begin{pmatrix} m_i I_{2\times 2} & A_i'(s_{r,i} + s_{\Delta,i} q_i) & A_i C_{1,i}^{\mathrm{T}} \\ (s_{r,i} + s_{\Delta,i} q_i)^{\mathrm{T}} A_i'^{\mathrm{T}} & J_{r,i} + J_{\Delta,i} & C_{2,i} + C_{3,i} q \\ C_1 A^{\mathrm{T}} & (C_{2,i} + C_{3,i} q_i)^{\mathrm{T}} & M_{h_i} \end{pmatrix},$$

$$f_i(t, w_i, \dot{w}_i) = \begin{pmatrix} A_i \left(s_{r,i} + s_{h_i} q\right) \dot{\theta}_i^2 - 2A_i' C_{1,i}^{\mathrm{T}} \dot{q}_i + f_{\mathrm{T},i}(\theta_i, t) \\ -2\left(C_{4,i} + M_{h_i} q_i\right) \dot{\theta} \dot{q}_i + f_{R,i}(q_i, t) \\ (C_{4,i} + M_{h_i} q_i)\dot{\theta}_i^2 - 2C_{3,i}\dot{\theta}_i \dot{q}_i - K_{h_i} q_i + l_{h_i} \end{pmatrix},$$

and those for the inner ring $M_{\mathrm{in}} = M_{h_{\mathrm{in}}}$ and $f_{\mathrm{in}} = K_{h_{\mathrm{in}}} q_{\mathrm{in}} + l_{h_{\mathrm{in}}}$.

The three bodies are coupled by unilateral constraints based on a contact model described in detail in Sec. 4 below. By introducing constraint forces the final system becomes an index-3 differential algebraic system of the generic form

$$M(w)\dot{w} \;=\; F(t, w, \dot{w}) - G_T(w)^{\mathrm{T}}\mu \tag{3}$$

$$0 \;=\; g_T(w) \tag{4}$$

with $G_T = \partial g / \partial w$.

## 3 Wavelet Element Method (WEM)

In [2] the general setting of the wavelet element method (WEM) is presented. Like in the finite element case it consists of a Galerkin semidiscretization with locally supported basis functions $\zeta_j$, but unlike finite elements the wavelet basis contains information which can be used in an effective way for system reduction. So an extra modal reduction step like in the FEM case is no longer required.

The discrete space $\mathcal{V}_0^h \subset \mathcal{V}_0$ is constructed by its basis functions $\zeta_j$ in the following way:

1. An appropriate father wavelet $\phi \in H^1(\mathbb{R})$ is selected, with the property that the translated functions $\phi(\cdot - j), j \in \mathbb{Z}$ are linearly independent and span a linear space $V_{n_0} \ldots \subset H^1(\mathbb{R})$

2. We consider father wavelet functions having compact support, so that by truncating the basis, dilating the basis functions and adding additional boundary wavelet functions a basis for a corresponding finite dimensional subspace of $H^1([0,1])$ can be constructed.

3. By forming tensor products of these basis functions a basis for $\breve{V}_{n_0} \subset H^1([0,1]\times[0,1])$ is obtained.

4. Finally by constructing a continuously differentiable map $F_\Omega : \Omega \longrightarrow [0,1]^2$ this basis can be transformed to a basis for $\mathcal{V}_0^h \subset H^1(\Omega)$

The selection of a father wavelet is based on the smoothness requirements given by the equations of motion (2). We choose the construction presented in [9] based on Daubechies wavelets of order $N$, [4], denoted as DB$N$ now on. An alternative basis is presented in [3] based on biorthogonal wavelets and can be used for more general geometries.

When scaling and translating father wavelet functions $\phi^{k,j} := \phi(2^k \cdot - j), j \in \mathbb{Z}, k \in \mathbb{Z}^+$ a basis of a higher dimensional space is constructed and a ladder of spaces is obtained

$$H^1(\mathbb{R}) \supset ... \supset V^n \supset V^{n-1} ... \supset V_{n_o}$$

giving a natural way of increasing or decreasing the resolution level $n$. The lowest possible resolution level is called $n_o$.

Following the steps 1-4 above a ladder of semidiscretization spaces is obtained:

$$H^1(\Omega) \supset ... \supset \breve{V}^n \supset \breve{V}^{n-1} ... \supset \breve{V}^{n_o}$$

with

$$\breve{V}^n := \operatorname{span}\left\{ \breve{\phi}^{n,j_1,j_2} : \breve{\phi}^{n,j_1,j_2} = \left(\phi^{n,j_1} \otimes \phi^{n,j_2}\right) \circ F_\Omega \right\}. \tag{5}$$

For the Galerkin ansatz function $u^h$ we set $\mathcal{V}_o^h = \breve{V}^n \oplus \breve{V}^n$ for some $n > n_o$ resulting in $N_q^2 = 2 \cdot 2^{2n}$ elastic degrees of freedom $q_j$.

In the following sections we formulate the model in this basis.

## 4 ELASTIC CONTACT

We consider now two bodies, the outer ring $\Omega_{\text{out}}$ and the roller $\Omega_{\text{R}}$ with boundary $\partial\Omega_{\text{out}} = \Gamma_1^{\text{out}} \cup \Gamma_0^{\text{out}}$ resp. $\partial\Omega_{\text{R}} = \Gamma_1^{\text{R}} \cup \Gamma_0^{\text{R}}$. Dirichlet boundary conditions are given on $\Gamma_0^i$ and Neumann boundary conditions on $\Gamma_1^i$.

The dynamic contact problem is to find at any time point $t$ a state $w(t)$ so that the two bodies are either in contact but not penetrating or are free floating. Contact causes contact forces as constraint forces, which are characterized by not being dragging forces.

The part of the Neumann boundary, where contact occurs will be denoted by $\Gamma_c^{\text{R}}$ rsp. $\Gamma_c^{\text{out}}$. These boundary segments depend on the actual state $w(t)$.

### 4.1 Determination of the contact points

The node-to-element approach by [6] considers the case, where the roller (called the slave body) penetrates the outer ring (called the master body). A penetrating nodal point is denoted by $\bar{x}_s \in \Gamma_1^{\text{R}}$.

For mathematically describing the contact condition we parameterize a section $\Gamma_c^{\text{R}} \subset \Gamma_1^{\text{R}}$ of the roller boundary and a corresponding section of the outer ring boundary $\Gamma_c^{\text{out}} \subset \Gamma_1^{\text{out}}$. This parametrization and the corresponding boundary description is based on the order of the discretization. If Daubechies wavelets DB3 are taken the interpolation error by describing these boundary segments by a third degree polynomial are of the same order as the overall discretization error.

We select the four nearest nodes to $\bar{x}_s$ on both boundaries and denote them by $x_{m_1}, x_{m_2}, x_{m_3}, x_{m_4}$ and $x_{s_1}, x_{s_2}, x_{s_3}, x_{s_4}$. The corresponding boundary profile sections of the undeformed bodies and the corresponding deformations can then be described by four third degree polynomials $x_s(\xi_s), u_s(\xi_s)$ and $x_m(\xi_m), u_s(\xi_m)$.

Let $\bar{\xi}_s$ and $\bar{\xi}_m$ be the parameter values of the (unknown) contact points, then we can formulate the contact conditions

$$g_{\text{con}}(w, \bar{\xi_m}, \bar{\xi_s}) = y_s + A(\theta_s)(x_s(\bar{\xi_s}) + u_s(\bar{\xi_s})) - (y_m + A(\theta_m)(x_m(\bar{\xi_m}) + u_m(\bar{\xi_m}))) = 0$$

Additionally we need the so-called non penetration condition

$$g_{npe}(w, \xi_m, \xi_s, \lambda) = \lambda A(\theta_s)(x_s'(\xi_s) + u_s'(\xi_s)) - A(\theta_m)(x_m'(\xi_m) + u_m'(\xi_m)) = 0$$

stating that the tangents at the contact points are parallel.

Together we get four conditions for the four unknown variables $\mu_s, \bar{\xi_s}, \bar{\xi_m}$ and the tangent scaling $\lambda$.

The corresponding constraint matrix $G$ is obtained by the requirement that the relative velocity in the contact points is orthogonal to the boundary normal vector in these points.

After having set up the constraints for all contact points we finally get a differential-

algebraic system of the following form

$$M(w)\dot{w} = F(t,w,\dot{w}) - G_T(w,\bar{\xi},\lambda)^{\mathrm{T}}\mu \quad (6)$$
$$0 = g_{\mathrm{con}}(w,\bar{\xi},\lambda) \quad (7)$$
$$0 = g_{\mathrm{npe}}(w,\bar{\xi},\lambda) \quad (8)$$

with $\xi \in \mathbb{R}^{2n_\mu}$ being the vector of all contact point parameters and $\lambda \in \mathbb{R}^{n_\mu}$ the vector of all tangent scaling variables.

This system has index-3 with $\lambda$ and $\bar{xi}$ as index-1 variables, while the Lagrange multipliers are index-3 variables. The numerical treatment of these kind of systems is discussed in [7, 1].

## 5 NUMERICAL SIMULATIONS

### 5.1 Numerical Algorithms

Before numerically integrating the system (6) its index has to be reduced to a stabilized index-2 system, [7, 1]. The resulting system can then be integrated by BDF methods like DASSL.

To handle switching between contact and no contact a switching function was implemented. This function is a vector valued function, with components corresponding to boundary nodal points. A zero of one of its components indicates the transition between the states contact/no contact has to be made. Zeros are detected by a safeguard algorithm based on inverse interpolation and bisection as described in [7].

To test the performance and accuracy of the wavelet ansatz we compare it with a corresponding FEM semidiscretization. The simulation, contact point detection and switching event handling is performed in both cases by identical algorithms.

### 5.2 Finite elements

FEMlab is used in plane stress mode to describe each individual body and compute mass and stiffness matrices $M_{h,in}, M_{h,R}, M_{h,out}, K_{h,in}, K_{h,R}$ and $K_{h,out}$ with linear elements. Typical triangularizations for the outer ring and the roller are depicted in Fig. 3. The boundary of the rolling elements are under Neumann boundary conditions. The outer boundary of the inner ring is under Neumann boundary conditions, as the inner boundary of the outer ring. Dirichlet boundary conditions are imposed at the outer boundary of the outer ring and inner boundary of the inner ring.

### 5.3 Wavelets

Own routines in Matlab were written for WEM. Typical wavelet triangularisations of the roller and rings are presented in Fig. 4. The Schwarz-Christoffel map is used to map the unit square to the circle, see [5]. The exponential map is used to map the unit square to the rings. The corresponding boundary conditions are periodic at two opposite sides of

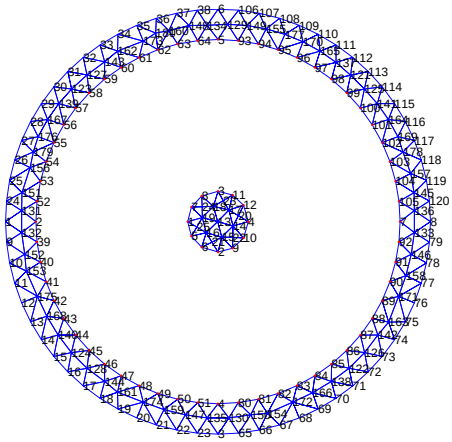

Figure 3: FEM triangularization of rolling elements and rings

the unit square and Dirichlet / Neumann conditions can be set at the other two. Wavelet DB3 was used in the discretization.

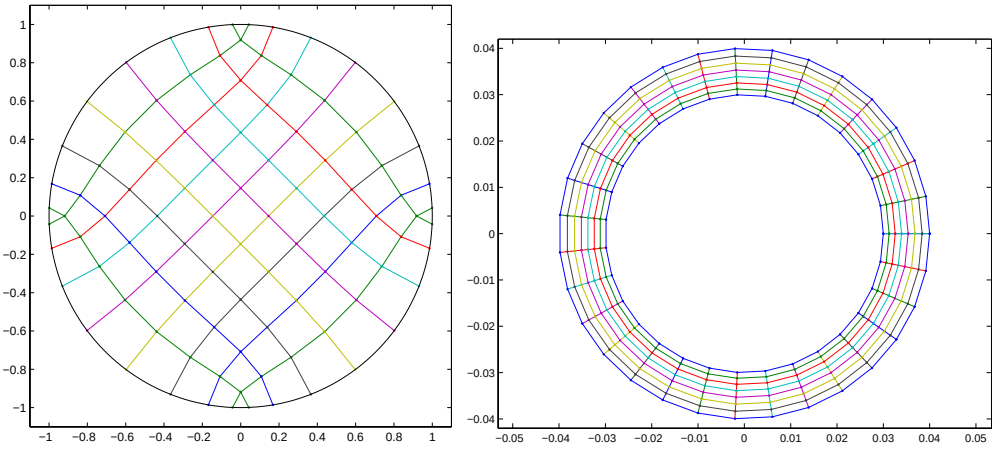


Figure 4: Wavelet triangularization of rolling elements and rings

### 5.4 Comparison WEM-FEM

We present in Fig. 5 the sparsity structure of $K_{h,R}$ of both approaches, FEM and WEM . The WEM stiffness matrix is always banded, with a bandwidth depending on size of the the wavelet support. This feature can be exploited to save computational work using specially adapted algorithms for banded matrices. FEM generates a sparse but unstructured stiffness matrix.

If $\rho$ is constant The mass matrix is the identity in the WEM case. This means that the spectrum is determined by the stiffness matrix $K_h$ only. This is not the case for a FEM

discretization.

Model reduction techniques reduce the number of elastic coordinates $q$ to $q_{red} = C_h q$ with some matrix $C_h \in \mathbb{R}^{N_{\text{red}} \times N_q}$. The mass and stiffness matrices are reduced by

$$M_{h,red} = C_h^{\mathrm{T}} M_h C_h$$

$$K_{h,red} = C_h^{\mathrm{T}} K_h C_h.$$

This matrix $C_h$ is in the FEM case obtained form the eigenvectors of the generalized eigenvalue problem

$$-\omega^2 M_h \tilde{q} = K_h \tilde{q}.$$

We perform model reduction by selecting eigenvectors corresponding to the $s$ lowest frequencies $\omega_1, \omega_2, ..., \omega_s$ and assembling them in $C_h = (\tilde{q}_1, \tilde{q}_2, ..., \tilde{q}_s)$.

In the WEM case the situation is different. We construct the matrix $C_h$ by setting to one the diagonal element corresponding to those wavelets that have the contact node in their support.

In Table 6.4 is the dimensions of the semidiscretisations with FEM, WEM and using WEM model reduction. Notice that the model reduction depends on the state and possible contact contraints applied at a certain time. We give the maximum number of equations selected by the algorithm for the time interval $[0, 0.1]$.

| | **FEM** | **WEM** | **red WEM** |
|---|---|---|---|
| **Roller** | 108 | 128 | max 40 |
| **Ex. Ring** | 976 | 2048 | max 128 |
| **In. Ring** | 480 | 512 | max 128 |

Table 1: Dimensions of the discretisations for FEM and WEM

In Fig. 7 we present the reference solution with FEM without model reduction and compare the step size sequence generated by DB3 and WEM model reduction. We observe that the WEM time step sizes are larger than those required by the FEM. Notice that the time points when the step size decreases drastically are those when the roller bounces against one of the rings. Although the number of equations in the reduced WEM model is considerably lower, the bounces occur at nearly the same instances. This property was not observed when using modal reduction.

In Fig. 6 the spectra of the roller element for FEM and WEM with and without model reduction are depicted. In the reduced WEM we observe that non determinant high frequency modes are removed, causing a significant speed-up of integration time.

## 6 CONCLUSIONS

We present a WEM discretisation of a simple 2D roller bearing model with possiblity to model reduction using the properties of wavelet decomposition.

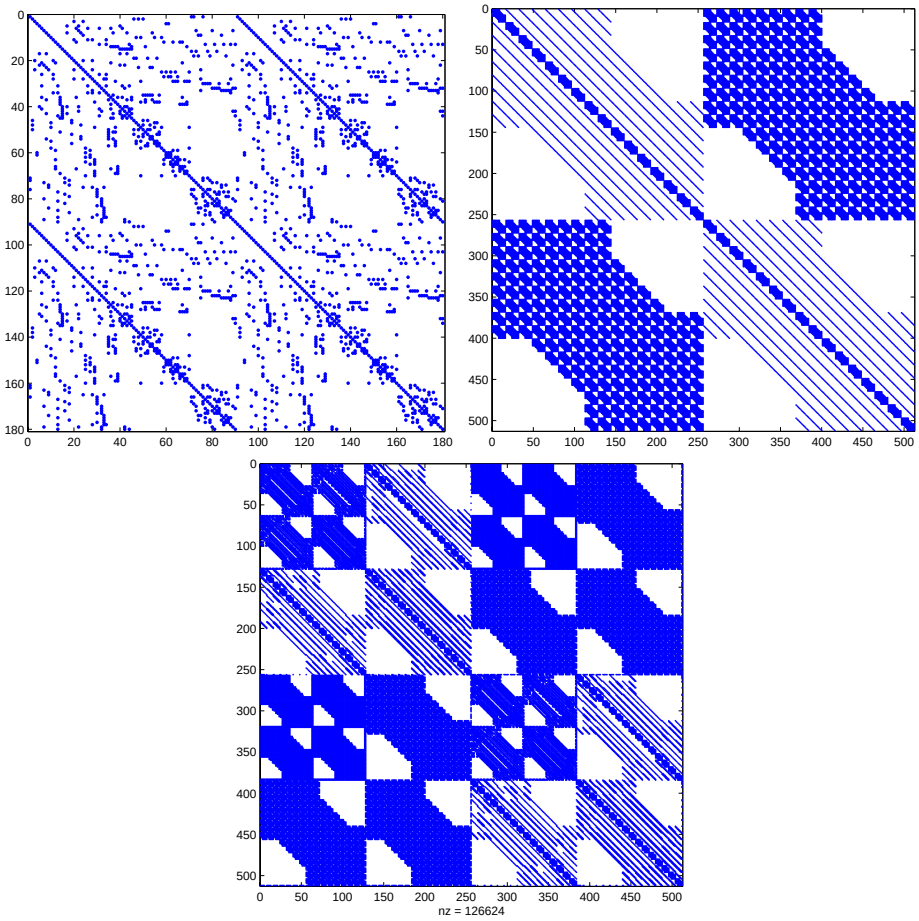


Figure 5: FEM and Wavelet (single and multiresolution) sparsity structure of stiffness matrices

We show that WEM model reduction techniques are robust in the sense that we do not need to know in advance where possible forces/interactions occur to apply modal reduction or static mode analysis.

An improvement with respect to linear FEM discretisation is shown.

We observe that the order of approximation of the boundary is the same, but WEM model reduction conserves this order after reduction.

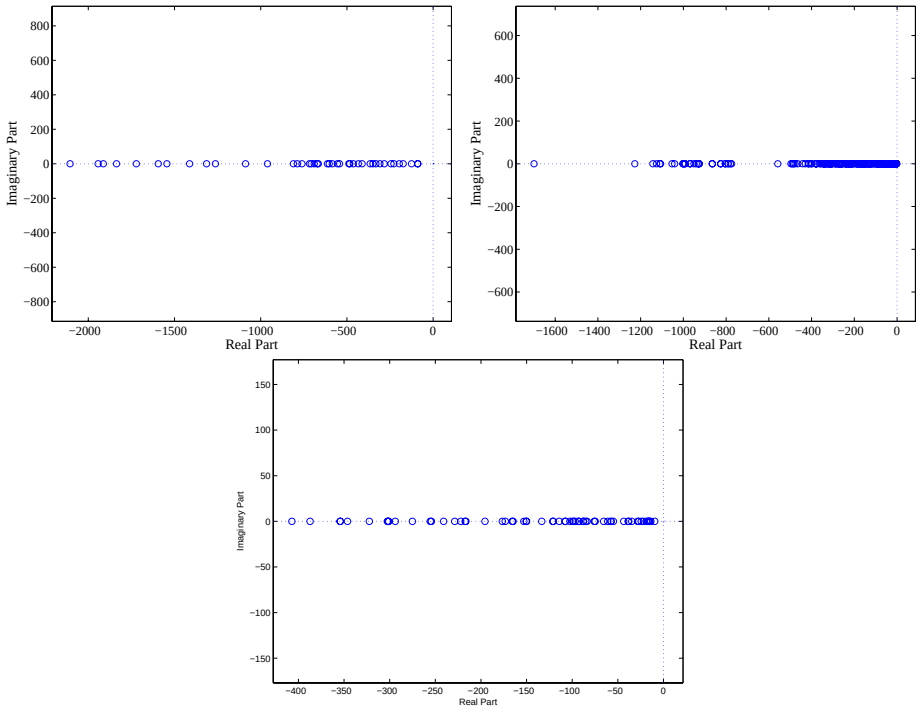


Figure 6: FEM and Wavelet spectrum of the stiffness matrix for the rolling element

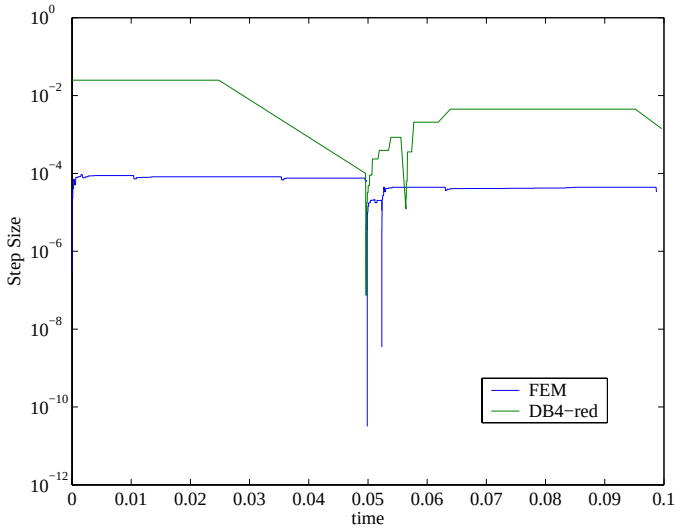


Figure 7: Step size sequence of the example

## REFERENCES


[1] Martin Arnold and Helmut Netter. Ein modifizierter Korrektor für die stabilizierte Integration diffenrential-algebraicher Systeme mit von Hessenberg abweichender Strucktur. Robotik und Systemdynamik (FF-DR) IB.Nr 515-93-03, DLR, DLR, Oberpfaffenhofen, 1993.

[2] Claudio Canuto, Anita Tabacco, and Karsten Urban. The wavelet element method. II. Realization and additional features in 2D and 3D. *Appl. Comput. Harmon. Anal.*, 8(2):123–165, 2000.

[3] Wolfgang Dahmen, Angela Kunoth, and Karsten Urban. Biorthogonal spline wavelets on the interval—stability and moment conditions. *Appl. Comput. Harmon. Anal.*, 6(2):132–196, 1999.

[4] Ingrid Daubechies. *Ten lectures on wavelets*. Society for Industrial and Applied Mathematics (SIAM), Philadelphia, PA, 1992.

[5] Tobin A. Driscoll. A MATLAB toolbox for Schwarz-Christoffel mapping. *ACM Trans. Math. Soft.*, (22):168–186, 1996.

[6] Peter Eberhard. Kontaktuntersuchungen durch hybride Mehrkörpersystem/ finite Elemente Simulationen. Berichte aus dem Machinenbau ISBN 3-8265-8107-5, Shaker Verlag GmbH, Aachen Germany, 2000.

[7] Edda Eich-Soellner and Claus Führer. *Numerical methods in multibody dynamics*. European Consortium for Mathematics in Industry. B. G. Teubner, Stuttgart, 1998.

[8] José Díaz López. A study on wavelet semidiscretization of elastic multibody systems. Licenciate Thesis 2002:4, Lunds Universitet, Numerisk Analys Box 117 SE-211 0 Lund Sweden, 2002.

[9] Pascal Monasse and Valérie Perrier. Orthonormal wavelet bases adapted for partial differential equations with boundary conditions. *SIAM J. Math. Anal.*, 29(4):1040–1065 (electronic), 1998.

[10] Bernd Simeon. *Numerische Simulation gekoppelter Systeme von partiellen und differential-algebraische Gleichungen in der Mehrkörperdynamik*. Fortschritt-Berichte VDI, 20,325, 2000.

[11] Anders Sjö. Numerical aspects in contact mechanics and rolling bearing simulation. Licenciate Thesis 1996, Numerisk Analys, Lunds Universitet, 1996.